Towards Procedures for Systematically Deriving Hybrid Models of Complex Systems

Pieter J. Mosterman[1] and Gautam Biswas[2]

[1] Institute of Robotics and Mechatronics, DLR Oberpfaffenhofen, P.O. Box 1116, D-82230 Wessling, Germany.
Pieter.J.Mosterman@dlr.de

[2] Department of Electrical Engineering and Computer Science, Box 1679 Sta B, Vanderbilt University, Nashville, TN 37235, U.S.A.
biswas@vuse.vanderbilt.edu

Abstract. In many cases, complex system behaviors are naturally modeled as nonlinear differential equations. However, these equations are often hard to analyze because of "stiffness" in their numerical behavior and the difficulty in generating and interpreting higher order phenomena. Engineers often reduce model complexity by transforming the nonlinear systems to piecewise linear models about operating points. Each operating point corresponds to a mode of operation, and a discrete event switching structure is added to implement the mode transitions during behavior generation. This paper presents a methodology for systematically deriving mixed continuous and discrete, i.e., *hybrid* models from a nonlinear ODE system model. A complete switching specification and state vector update function is derived by combining piecewise linearization with singular perturbation approaches and transient analysis. The model derivation procedure is then cast into the phase space transition ontology that we developed in earlier work. This provides a systematic mechanism for characterizing discrete transition models that result from model simplification techniques. Overall, this is a first step towards automated model reduction and simplification of complex high order nonlinear systems.

1 Introduction

Systems and control engineers often apply simplification techniques when modeling and analyzing complex physical systems that include components like valves, pumps, and diodes, and phenomena such as friction effects [3]. To avoid complex nonlinearities and stiffness caused by steep slopes in the behavior, these components are modeled to exhibit switching behavior. This results in the overall system model generating piecewise continuous behaviors and discrete transitions, i.e., *hybrid* behaviors. *Hybrid automata* [1] have been employed as a computational mechanism for implementing these models, with a discrete control structure defining the switching between *modes* or states of the automata. Each mode has an associated set of ordinary differential equations (ODEs) that governs continuous behavior evolution in that mode. Events associated with the

mode switching generate *actions* that may produce discontinuous changes in state variables.

Consider the hydraulic actuator illustrated in Fig. 1. The valve at the top of the cylinder controls oil flow into and out of the cylinder, and the flow rate is a function of the control pressure p_{in}. The flow of oil determines the position of the piston in the cylinder, and this in turn determines the position of the load, e.g., the elevator control surface of an airplane. To prevent damage to the actuator system, a relief valve on the left side of the cylinder opens when the pressure in the cylinder exceeds a certain value.

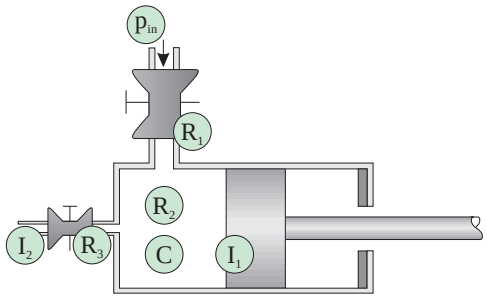

Fig. 1. Model parameters of a hydraulic actuator.

If the valve behaviors are approximated and simplified to be discrete, the actuator can be modeled as a hybrid automata with four states: α_{00}, both valves closed, α_{01}, relief valve open and control valve closed, α_{10}, control valve open and relief valve closed, and α_{11}, both valves open. The dynamic behavior in each of these modes can be derived from the actuator parameters, that include R_1, the resistance of the open control valve, R_2, the internal dissipation parameter for the oil, R_3, the resistance of the open relief valve, C, the oil elasticity, I_1, the piston inertia, and I_2, the relief valve fluid inertia.

System modelers often employ simplification techniques that involve dropping very small and very large parameters that do not play a significant role in gross system behavior. Applying this approach to the actuator system, parameters associated with the oil, R_2 and C, may be removed to reduce the order of the system model. For the simplified model, the dynamic behavior models for the different modes are given in Table 1, where f_1 is the piston velocity and f_2 is the fluid flow rate through the relief valve. The control valve and the relief valve are the two components in the actuator that are modeled to have discrete transitions from open to closed, and vice versa. An external control variable, u_v, determines the opening and closing of the control valve (e.g., the valve is closed when $u_v < 0$). The relief valve opens when $p > p_{th}$.

For mode α_{00}, there is no oil flow into the cylinder, therefore, the entry action, i.e., the initial conditions that have to be satisfied on entry into this mode, includes the constraint, $f_1 = 0$. The entry action for mode α_{01} is more compli-

Table 1. Mode specification table.

mode	$\dot{x} = f(x,u)$	entry action
α_{00}	$\dot{f_1} = 0$ $\dot{f_2} = 0$	$f_1 = 0$ $f_2 = 0$
α_{01}	$\dot{f_1} = -\frac{R_3}{I_1+I_2} f_1$ $\dot{f_2} = -\frac{R_3}{I_1+I_2} f_2$	$f_1 = \frac{1}{I_1+I_2}(I_1 f_1 - I_2 f_2)$ $f_2 = \frac{1}{I_1+I_2}(I_1 f_1 - I_2 f_2)$
α_{10}	$\dot{f_1} = p_{in} - \frac{R_1}{I_1} f_1$ $\dot{f_2} = 0$	$f_2 = 0$
α_{11}	$\dot{f_1} = \frac{1}{I_1}(p_{in} - R_1(f_1 + f_2))$ $\dot{f_2} = \frac{1}{I_2}(p_{in} - R_1(f_1 + f_2) - R_3 f_2)$	

cated. In this mode, f_1 and f_2 are algebraically related ($f_1 = -f_2$). The initial values for f_1 and f_2 have to be initialized using this constraint, but one equation is not sufficient to solve for their values. Additional constraints presented in Section 5 are used to define the entry action listed in Table 1.

In the past, engineers have used *ad hoc* approaches to handle transitions between piecewise models, however, even for the simple example above this may lead to incorrect model definitions. In Section 5 systematic analysis shows that the entry actions as specified in Table 1 are incomplete, and demonstrates how the correct state mapping as derived by a structured approach is much more complex. This shows that deriving the correct event structures and corresponding actions at mode transitions is more involved for systems with complex interactions among their subsystems.

This paper develops a structured approach to analyzing complex nonlinear models, applying systematic abstraction and simplification mechanisms to create simpler multiple piecewise continuous models. The price we pay in achieving this reduction is the introduction of complex discrete components in the hybrid model of the system. The two main steps in this procedure are illustrated in Fig. 2. We start with the complex continuous nonlinear model of the system. Step 1 applies simplification techniques to convert the nonlinear models to simpler piecewise continuous (possibly linear) behavior models. The result is a hybrid model whose state variable values are continuous, but the time derivatives may be discontinuous. This is equivalent to a C^0 hybrid model with sets of differential equations defining the behaviors in individual modes, and a function, γ, that defines transitions between the modes. Step 2 applies techniques like *singular perturbation* [3] and *eigenvalue analysis* [8] that remove large and small parameters from the models, and thus eliminate steep transitions in the behaviors within modes. The resultant models combine three components: (i) a reduced order ODE model, f, (ii) the discrete event mode transition function, γ, and (iii) the state transition function, g, that captures the discontinuous state variable value changes between modes.

The derivation process for g can be described by two basic actions in hybrid models of physical systems:

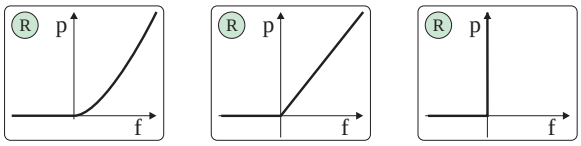

Fig. 2. Abstraction levels.

1. a *manifold projection* that results from the generated algebraic constraints, and
2. an *aborted projection* because detailed continuous projection behavior causes further discrete changes.

We use this framework to derive a computational model of the resulting hybrid system as a hybrid automata extended with branch points (junctions) to model the immediate consecutive discrete events and actions. A phase space analysis illustrates these concepts, and allows us to relate the results back to an ontology of phase space transition behavior presented in previous work [6].

2 The Approach

Consider a nonlinear system with state equations of the form

$$\dot{x} = A(x)x + B(x)u. \tag{1}$$

System designers and analysts often simplify the above model by identifying operating regions of interest within the behavior space, called *modes*. Such modes may be the result of design decisions, e.g., the take-off, cruise, and landing modes of aircraft fly-by-wire systems, or determined from component models that make up the system, e.g., by taking into account the open and closed states of the valves in the actuator system. Modes can also be identified by the discrete control actions of supervisory controllers. Along with mode identification, transitions between modes, α, are also defined (cf. Table 1). Most often, the purpose for breaking up complex behaviors into modes of operating regions is so that the system model can be linearized within each mode, i.e.,

$$f_{\alpha_i} : \dot{x} = A_{\alpha_i}x + B_{\alpha_i}u. \tag{2}$$

The result is a set of piecewise models that together define the behavior space of interest, with transition conditions between pairs of modes, α_i and α_{i+1} given by the function

$$\gamma_{\alpha_i}^{\alpha_{i+1}} : C_{\alpha_i}x + D_{\alpha_i}u > 0. \tag{3}$$

Model reduction techniques, such as singular perturbation and eigenvalue based techniques, are readily applicable to the linearized systems. They provide systematic methodologies to reduce the order of each piecewise model. Applying

singular perturbation, a small parameter, ϵ, is removed from the model by letting its value tend to 0. This requires the formulation

$$\begin{array}{ll} f_{\alpha_i} & : \dot{x} = A_{\alpha_i}(\epsilon)x + B_{\alpha_i}(\epsilon)u \\ \gamma_{\alpha_i}^{\alpha_{i+1}} & : C_{\alpha_i}(\epsilon)x + D_{\alpha_i}(\epsilon)u > 0. \end{array} \tag{4}$$

In this formulation, slow and fast variables can be separated according to

$$f_{\alpha_i} : \begin{cases} \dot{y} = A^y_{\alpha_i}(\epsilon)x + B^y_{\alpha_i}(\epsilon)u \\ \epsilon\dot{z} = A^z_{\alpha_i}(\epsilon)x + B^z_{\alpha_i}(\epsilon)u. \end{cases} \tag{5}$$

Making $\epsilon \to 0$ leads to equations of the form $z = f(y, u)$. Assuming that the system of algebraic equations is non singular, z can be substituted in the equation for $\dot{y}$ to derive an explicit reduced order ODE system. However, if $\epsilon \to 0$ leads to a singular solution, $0 = f(y, u)$, system behavior is now defined by an implicit system of differential and algebraic equations (DAE), and the variable vector y may also include a fast component. In the limit, this fast behavior is replaced by an instantaneous projection $y^+ = g_{\alpha_{i+1}}(y, u)$, where y^+ is the initial value in mode α_{i+1}, $y^0_{\alpha_{i+1}} = y^+$, and y is the value of the reduced order system in mode α_i when $\gamma_{\alpha_i}^{\alpha_{i+1}} > 0$ was first satisfied.

Similarly, when the system of equations becomes singular for $\epsilon \to 0$, a state vector transformation may be required to achieve the desired separation and this may require a projection, $g_\alpha(x, u)$. We discuss this in greater detail in Section 5. In general, it may be difficult to derive the transformation by analytic methods. Information about the physical system can be invoked to assist in deriving the solution. The projection can be found by boundary behavior analysis of the detailed model, i.e., with the ϵ parameter. As an alternative, or if this detailed model is not available, the projection can be computed by integrating the instantaneous field dynamics [4] and by subspace iteration [7]. These are implementations based on the use of the reducing subspaces of the Kronecker Canonical Form [2] to capture the state projection.

The resulting model contains the reduced order specification of continuous behavior, f, the transition conditions, γ, and the projection equations, g,

$$\begin{array}{ll} f_{\alpha_i} & : \dot{y} = A'_{\alpha_i} y + B'_{\alpha_i} u \\ \gamma_{\alpha_i}^{\alpha_{i+1}} & : C'_{\alpha_i} y + D'_{\alpha_i} u > 0 \\ g_{\alpha_{i+1}} & : y^0_{\alpha_{i+1}} = E_{\alpha_{i+1}} y + F_{\alpha_{i+1}} u \end{array} \tag{6}$$

We study the effects of the order reduction technique on the state vector transfer function and transition conditions in this paper. Detailed analysis may be required when variables that constitute the γ function exhibit impulsive behavior. To identify such behavior, γ can be expressed in terms of $\dot{y}$. If any of the variables in the y vector are part of the algebraic constraints that develop when $\epsilon \to 0$, they produce impulses. Detailed study may reveal the need for an additional transition modes to be introduced in the mode transition behavior. This transitional mode exists only at a point in time, and has no specification for continuous behavior. Furthermore, some transitional modes may have no effect on the state vector. In previous work, we termed these transitional modes

pinnacles and *mythical modes*, respectively. A phase space analysis conducted in this paper establishes the relation between this approach and our established ontology for phase space transition behavior [6].

3 A Piecewise Model

In a nonlinear continuous ODE model of the hydraulic actuator, the nonlinear characteristics of the externally controlled valve and the relief valve can be modeled as shown in Fig. 3. Including the oil parameters (R_2 and C) results in the fifth order nonlinear ODE

$$\begin{bmatrix} \dot{f}_1 \\ \dot{f}_2 \\ \dot{p}_1 \\ \dot{s}_1 \\ \dot{s}_2 \end{bmatrix} = \begin{bmatrix} \frac{-R_1(s_1)R_2}{D_1} & \frac{-R_1(s_1)R_2}{D_1} & \frac{R_1(s_1)}{D_1} & 0 & 0 \\ \frac{-R_1(s_1)R_2}{D_2} & \frac{-R_1(s_1)R_2 - R_3(p,s_2)(R_1(s_1)+R_2)}{D_2} & \frac{R_1}{D_2} & 0 & 0 \\ \frac{-R_1}{D_3} & \frac{-R_1(s_1)}{D_3} & \frac{-1}{D_3} & 0 & 0 \\ 0 & 0 & 0 & 0 & 0 \\ 0 & 0 & 0 & 0 & 0 \end{bmatrix} \begin{bmatrix} f_1 \\ f_2 \\ p_1 \\ s_1 \\ s_2 \end{bmatrix} + \begin{bmatrix} \frac{R_2 p_{in}}{D_1} \\ \frac{R_2 p_{in}}{D_2} \\ \frac{p_{in}}{D_3} \\ u_v \\ u_r \end{bmatrix} \tag{7}$$

with $D_1 = I_1(R_1(s_1) + R_2)$, $D_2 = I_2(R_1(s_1) + R_2)$, and $D_3 = C(R_1(s_1) + R_2)$. The variable u_v is externally controlled, and $u_r = \frac{1}{1+e^{-a(|p|-p_{th})}}$ represents a function that approaches a step when $a \to \infty$. The two state variables, s_1 and s_2, provide a parametric representation model for the detailed continuous switching behavior of the two valves. The cylinder oil pressure, p, expressed in terms of the state variables, is:

$$p = \frac{R_1}{R_1 + R_2}(p_1 + \frac{R_2}{R_1}p_{in} - R_2(f_1 + f_2)). \tag{8}$$

When p approaches $\pm p_{th}$, u_r becomes positive and the valve opens by switching to another behavior dimension ($s_2 > 0$). Since u_r is always positive, the valve does not close, once it is opened. Therefore, transitions from α_{01} to α_{00} and α_{10} are not defined in Table 2. For the same reason, there are no transitions from α_{11} to α_{00} and α_{10}.

Piecewise linearization of $R_1(s_1)$ and $R_3(p, s_2)$ into regions of high resistance, $R_{i,h}$, and low resistance, $R_{i,l}$, is defined as:

$$\begin{aligned} R_1 &= \text{ if } (u_v < 0) \text{ then } R_{1,h} \text{ else } R_{1,l} \\ R_3 &= \text{ if } (R_3 = R_{3,l} \text{ or } p > p_{th}) \text{ then } R_{3,l} \text{ else } R_{3,h} \end{aligned} \tag{9}$$

This allows for removal of the states s_1 and s_2 from the system model, resulting in a linear ODE model with four global modes: $\alpha_{00} \to \{R_{1,h}, R_{3,h}\}$, $\alpha_{01} \to \{R_{1,h}, R_{3,l}\}$, $\alpha_{10} \to \{R_{1,l}, R_{3,h}\}$, and $\alpha_{11} \to \{R_{1,l}, R_{3,l}\}$. The transitions between the modes are specified in Table 2.

4 From Complex to Simpler ODEs

The parameters $R_{1,h}$ and $R_{3,h}$ in the piecewise models are large compared to the other system parameters. The singular perturbation approach can be applied to

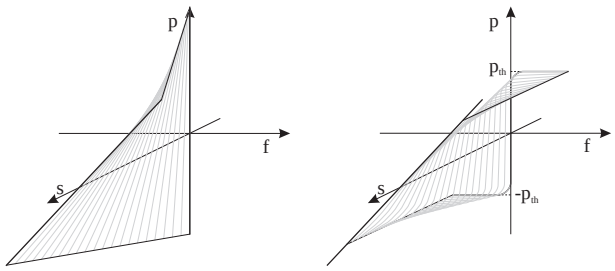

(a) controlled valve (b) pressure relief valve

Fig. 3. Nonlinear valve resistance characteristics.

Table 2. Mode transition table.

present mode	next mode			
	α_{00}	α_{01}	α_{10}	α_{11}
α_{00}		$p > p_{th}$	$u_v > 0$	$p > p_{th} \wedge u_v > 0$
α_{01}				$u_v > 0$
α_{10}	$u_v < 0$	$u_v < 0 \wedge p > p_{th}$		$p > p_{th}$
α_{11}		$u_v < 0$		

remove these large parameters ($R_{1,h} \to \infty$ and $R_{3,h} \to \infty$) and arrive at simpler reduced order ODEs for each mode. To simplify notation, we set $R_1 = R_{1,l}$ and $R_3 = R_{3,l}$. The dynamic behavior in α_{01} is derived by $R_{1,h} \to \infty$ and can be expressed as:

$$f_{\alpha_{01}} : \begin{bmatrix} \dot{f}_1 \\ \dot{f}_2 \\ \dot{p}_1 \end{bmatrix} = \begin{bmatrix} -\frac{R_2}{I_1} & -\frac{R_2}{I_1} & \frac{1}{I_1} \\ -\frac{R_2}{I_2} & -\frac{R_2+R_3}{I_2} & \frac{1}{I_2} \\ -\frac{1}{C} & -\frac{1}{C} & 0 \end{bmatrix} \begin{bmatrix} f_1 \\ f_2 \\ p_1 \end{bmatrix} \tag{10}$$

From Table 2 it is clear that this abstraction does not affect the switching constraints that define further discrete transitions out of this mode. The only transition out of this mode, $\alpha_{01} \to \alpha_{11}$, is governed by the external variable u_v ($u_v > 0$).

For α_{10}, $R_{3,h} \to \infty$ implies $f_2 = 0$ and behavior reduces to a second order system

$$f_{\alpha_{10}} : \begin{bmatrix} \dot{f}_1 \\ \dot{p}_1 \end{bmatrix} = \begin{bmatrix} -\frac{R_1 R_2}{I_1(R_1+R_2)} & \frac{R_1}{I_1(R_1+R_2)} \\ -\frac{R_1}{C(R_1+R_2)} & -\frac{1}{C(R_1+R_2)} \end{bmatrix} \begin{bmatrix} f_1 \\ p_1 \end{bmatrix} + \begin{bmatrix} \frac{R_2}{I_1(R_1+R_2)} \\ \frac{1}{C(R_1+R_2)} \end{bmatrix} \begin{bmatrix} p_{in} \end{bmatrix}. \tag{11}$$

In both modes, the pressure, p, in the switching condition is given by Eq. (8). The reduced behavior in α_{00} is given by an autonomous second order system

$$f_{\alpha_{00}} : \begin{bmatrix} \dot{f}_1 \\ \dot{p}_1 \end{bmatrix} = \begin{bmatrix} -\frac{R_2}{I_1} & \frac{1}{I_1} \\ -\frac{1}{C} & 0 \end{bmatrix} \begin{bmatrix} f_1 \\ p_1 \end{bmatrix}. \tag{12}$$

Introducing $R_{1,h} \rightarrow \infty$ into Eq. (8), results in this pressure, p, being expressed as

$$p = p_1 - R_2 f_1 > p_{th}. \tag{13}$$

It turns out that the spread of the eigenvalues in these linearized, simplified, and reduced systems of equations is still quite large. For example, given parameter values, $R_{1,l} = R_{3,l} = 0.01$, $R_2 = 100$, $C = 5 \cdot 10^{-6}$, $I_1 = 1$, and $I_2 = 0.01$, one of the eigenvalues is computed to be five orders of magnitude less than the others in the modes α_{01} and α_{10}. This implies that the system still operates at two widely differing time scales, and it may be possible to simplify the system model further by abstracting the R_2 and C parameters. Applying this change will affect the state variable p_1, which is part of the switching condition, $p > p_{th}$. This requires a detailed study of the switching characteristics.

5 The State Mapping

The application of singular perturbation methods to the model in the last section with $\frac{1}{R_2}$ and C as the small parameters, replaces some differential equations by algebraic constraints. For example, the α_{01} mode is reduced from a 3^{rd} order to a 1^{st} order system, whereas mode α_{00} is reduced from a 2^{nd} to a 0^{th} order (purely algebraic) system. This may cause state variable values to change discontinuously during mode transitions.

5.1 Jump into mode α_{01}

When $R_2 \rightarrow \infty$, Eq. (10) becomes a singular system of equations with $-f_1 - f_2 = 0$. In phase space, this algebraic relation constitutes a manifold to which behavior is confined. The dynamic system behavior on this manifold is derived by applying a transformation, $x = I_1 f_1 - I_2 f_2$, which gives $\dot{x} = R_3 f_2$. Substituting for $f_1 (= -f_2)$ in the expression for x and eliminating f_2 yields

$$\dot{x} = -\frac{R_3}{I_1 + I_2} x. \tag{14}$$

If mode α_{01} is entered at a point not on this manifold, an instantaneous projection in the impulse space has to be executed to satisfy the manifold constraint. The impulse space can be derived by integrating the dynamic behavior in Eq. (14) over an infinitesimal interval from t to t^+, which gives $I_1(f_1^+ - f_1) - I_2(f_2^+ - f_2) = 0$ [4]. Combined with the manifold constraint at t^+, $f_1^+ = -f_2^+$, this computes the projection to be

$$g_{\alpha_{01}} : f_1^+ = \frac{1}{I_1 + I_2}(I_1 f_1 - I_2 f_2). \tag{15}$$

Table 2 shows that the transition conditions for α_{01} are not affected by the variables f_1 and f_2, therefore, no further analysis is required.

5.2 The Jump into mode α_{00}

In mode α_{00}, $R_2 \to \infty$ produces $f_1 = 0$. Again, this constitutes a manifold in phase space and transition into α_{00} requires a projection,

$$g_{\alpha_{00}} : f_1^+ = 0. \tag{16}$$

However, analysis of the detailed model indicates that the switching condition from mode α_{00} to mode α_{01} in Eq. (13) may be activated before f_1 becomes 0. Therefore, this transition condition needs to be analyzed more precisely.

When $R_2 \to \infty$, the switching condition in Eq. (13) becomes singular, and the value for p cannot be determined from the state variables. Therefore, p has to be expressed in terms of the time derivatives of the states. For this system, Eqs. (12) and (13) yield, $p = \frac{1}{I_1}\dot{f}_1$. The $f_1 = 0$ constraint corresponds to a discontinuous change in f_1, therefore, $\dot{f}_1$ may produce an impulse.

Impulse behavior is too coarse an approximation of the underlying detailed continuous transient. A more refined analysis solves the detailed differential equation in the time domain. The characteristic polynomial of $f_{\alpha_{00}}$ has two roots

$$\lambda_{1,2} = \frac{1}{2I_1}(-R_2 \pm \sqrt{R_2^2 - \frac{4I_1}{C}}). \tag{17}$$

Assuming complex eigenvalues[1] ($\lambda_{1,2} = \lambda_r \pm j\lambda_i$), the pressure variable in mode α_{00} is ($t_0 = 0$ for notational convenience)

$$p_1(t) = e^{\lambda_r t}(p_1(0)cos(\lambda_i t) + \frac{1}{\lambda_i}(\dot{p}_1(0) - \lambda_r p_1(0))sin(\lambda_i t)). \tag{18}$$

Applying a third order Taylor series approximation yields ($\dot{p}_1 = -\frac{1}{C}f_1$),

$$p_1(t) = (1 + \lambda_r t + \frac{\lambda_r^2 t^2}{2})(p_1(0)(1 - \frac{(\lambda_i t)^2}{2}) + (-\frac{f_1(0)}{C} - \lambda_r p_1(0))t). \tag{19}$$

The switching condition is based on $p = p_1 - R_2 f_1(t)$, where $f_1(t)$ is used instead of $f_1(0)$ because the value of f_1 changes during the time interval in which $p_1(t)$ rises and it may be different from $f_1(0)$ when $p(t)$ reaches p_{th}.

This condition can be used to check if $p > p_{th}$, and if so, the time, $t_s = f_t(p_1, f_1, p_{th})$, at which this constraint becomes true. This value can then be used in the expression for f_1 to derive the discontinuous change upon switching. Abbreviating $f_1(0)$ and $p_1(0)$ as f_1 and p_1, respectively, and using $a = (-\frac{f_1}{C} - \lambda_r\frac{p_1 + f_1 R_2 R_2}{I_1} - \frac{p_1 R_2}{I_1} + \lambda_r R_2 f_1)/\lambda_i$, $b = p_1 - R_2 f_1$, and $c = -p_{th}$, the solution is given by

$$t_s = \frac{-(b-c)}{a\lambda_i + c\lambda_r} + \frac{\frac{1}{2}c(\lambda_r^2 + \lambda_i^2)(b-c)^2}{(a\lambda_i + c\lambda_r)^3}. \tag{20}$$

Substituting t_s in the expression for $f_1(t)$ in α_{00} results in the state mapping

$$g_{p,\alpha_{00}} : f_1^+ = e^{\lambda_r t_s}(f_1 cos(\lambda_i t_s) + (-\frac{R_2}{I_1}f_1 + \frac{p_1}{I_1} - \lambda_r f_1)\frac{sin(\lambda_i t_s)}{\lambda_i}), \tag{21}$$

[1] Analysis of real eigenvalues is similar.

where $f_1 = f_1(t_0)$ and f_1^+ the value of f_1 when α_{00} is exited because $p > p_{th}$.

This is graphically depicted in Fig. 4 for a third and fourth order Taylor approximation of f_1, $f_1^{p,3}$ and $f_1^{p,4}$, respectively.[2] Here an initial positioning maneuver of the piston is aborted at t_0, which causes the relief valve to open at t_s. The error between the third and fourth order approximations is shown by ϵ_3 and ϵ_4, respectively.

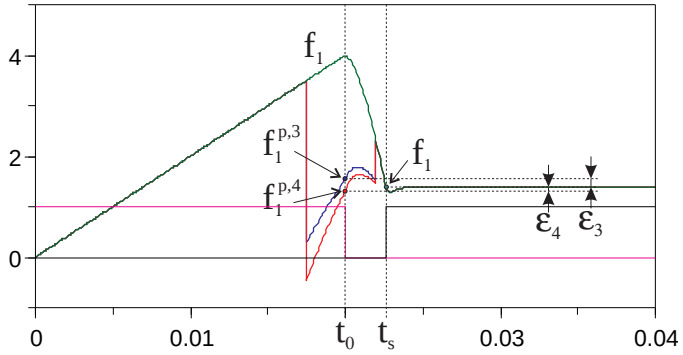

Fig. 4. Value of f_1 at t_s for a detailed model and its predictions at t_0.

5.3 A Computational Model

The discrete transition model that results from the abstractions of the detailed continuous behavior can be modeled by the extended hybrid automata structure in Fig. 5. The traditional hybrid automata is extended by junctions (indicated by small circles). When an event triggers a transition to a junction, the events on each of the exiting transitions from the junction are evaluated, resulting in an immediate second transition.

In this model, when the external control valve closes ($u_v < 0$), the time t_s at which the relief valve opens is computed by $f_t(p_1, f_1, p_{th})$ using the detailed continuous transient. If this computation returns a value $t_s \geq 0$, control is switched to the lower branch, else control switches to the branch at the right. This last branch indicates that the system moves to the field description for α_{00}, and, therefore, requires a consistent projection of the state variables (i.e., $f_1 = 0$). If the lower branch is taken, first the effect of the quick pressure build-up and corresponding flow decrease has to be accounted for by executing $f_1 = g_{p,\alpha_{00}}(f_1, p_1, t_s)$. This results in a new value for f_1 when the continuous behavior in α_{01} is activated. Again, behavior in this mode is subject to manifold constraints, and the corresponding projection $f_1 = g_{\alpha_{01}}(f_1, f_2)$ takes place

[2] The predictions are computed during a short time interval around t_0 to avoid singularities that exist over the entire range. Note that the values only need to be computed at t_0.

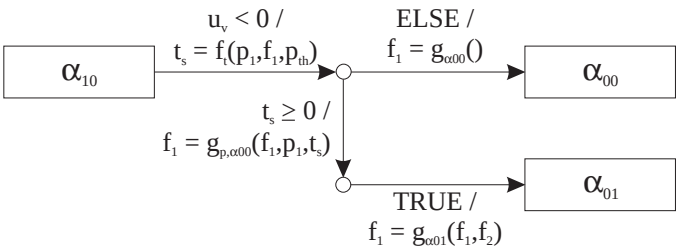

Fig. 5. Complex discrete switching structure.

before α_{01} is activated to ensure values are consistent in this mode. Note that in α_{01}, p_1 is not a state variable but derived from $p_1 = p_{in} - f_1 R_1$. Further, the systematically derived control structure is more complex as compared to the transitions in Table 2.

6 Phase Space Transition Behavior

The mode and discontinuous state changes can now be characterized in terms of a phase space transition ontology. In other work [6], three principal transition functions were analyzed in phase space: (i) transition to a mythical mode, (ii) transition to a pinnacle, and (iii) transition to a continuous mode.

When switching to α_{00}, the two possible scenarios are

1. $p < p_{th}$ in which case a projection of f_1 onto $f_1 = 0$ occurs, and the system remains in α_{00}. This represents a transition to a *continuous* mode.
2. $p \geq p_{th}$ in which case
   - there may be a distinct drop in f_1 before switching to α_{01}. This is a transition to a *pinnacle*, or
   - the switch to α_{01} has occurred before any significant change in f_1 occurs. This represents a transition to a *mythical mode*.

The switch to α_{01} may also include a discontinuous state change because of the manifold projection that immediately follows the pinnacle or mythical mode.

Figure 6 shows the phase space transition behavior for two values of C in a C^0 hybrid model with parameter values $R_{1,l} = R_{3,l} = 0.01$, $R_{1,h} = R_{3,h} = 1{\cdot}10^7$, $R_2 = 100$, $I_1 = 1$, $I_2 = 0.01$, and $p_{th} = 1000$. Velocity f_1 is plotted on the x-axis and pressure p is plotted on the y-axis. The discontinuous approximations are superimposed by dotted lines.[3] When the control valve closes, f_1 has value 4, and the pressure in the cylinder starts to rise quickly (Fig. 4 depicts the time domain behavior). This behavior consists of an immediate change in p caused by the term $f_1 R_2$, and a quick continuous change because of the pressure build up.

[3] These approximations are not simulation results.

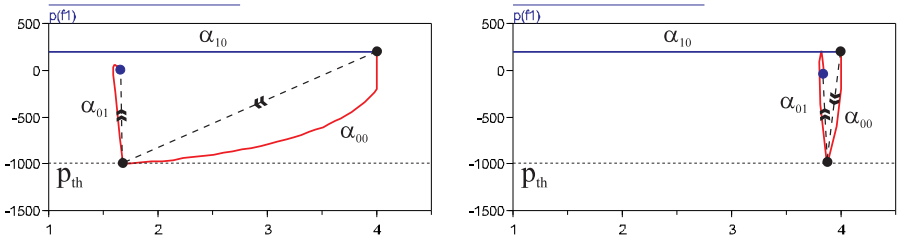

(a) $C = 1 \cdot 10^{-5}$ (b) $C = 1 \cdot 10^{-6}$

Fig. 6. Dominant C phase space switching behavior.

If the absolute pressure exceeds 1000, the mode switch to α_{01} occurs. In this mode, there is another quick change in f_1, this time governed by the dependency between I_1 and I_2. Because I_1 is several orders of magnitude larger than I_2, only a small change in f_1 occurs. The interaction between the three state variables in the C^0 hybrid model, f_1, f_2, and p_1, causes oscillatory behavior in α_{01}. This is clearly seen in Fig. 6(b). The discontinuous jump does not include this behavior, but immediately reaches the final value. The phase space behaviors present examples of two consecutive discontinuous state variable value changes that are of different types. The intermediate value of f_1 is achieved in a pinnacle mode, and the final value is governed by a manifold projection. Note that the pinnacle is crucial in computing the correct final value of the variable in α_{01}, when continuous behavior resumes.

If $R_2 > 250$, $f_1 R_2$ becomes the dominant factor in the phase space transition behavior, as shown in Fig. 7 for $C = 1 \cdot 10^{-5}$ and $R_2 = 500$. The consecutive switch to α_{01} follows immediately after the switch to α_{00}. As a consequence, α_{00} does not affect the value of f_1, therefore, this is a mythical mode. Mode α_{00} is not intrinsically a mythical mode because the state variable values when the mode is entered determine whether it is exited immediately. Only in such situations mythical behavior occurs. The projection in α_{01} that follows is shown more clearly in Fig. 7(b) for a larger value of I_2. For these parameters, Eq. (15) verifies the value $f_1^+ = 2$ ($f_1 = 4$, $f_2 = 0$) and confirms that larger values of I_2 have a greater effect on the magnitude change of f_1. Again, the fast oscillatory behavior of the manifold projection is abstracted away in the discontinuous approximation.

7 Conclusions

This paper shows how nonlinear and high order system models can be systematically reduced to piecewise linear systems with more uniform time scales of behavior. The resultant hybrid model is obtained in two steps: (i) C^0 continuous with piecewise simpler behavior and switching conditions, and (ii) piecewise

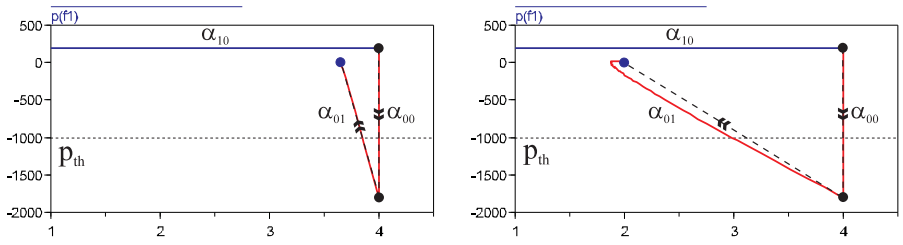

(a) $I_2 = 0.1$ (b) $I_2 = 1$

Fig. 7. Dominant R_2 phase space switching behavior.

continuous reduced order behavior with switching conditions and discontinuous changes in state variable values. The reduction in continuous domain complexity is gained at the cost of increasingly complex discrete event control structures. Because of the intricacies in defining the switching conditions and the corresponding jumps in the variable values, *ad hoc* modeling schemes can often produce erroneous results. This is most likely to happen when jumps occur in state variable values, caused by the introduction of algebraic constraints. The manifold projections that result may be aborted because intermediate variable values derived from the detailed dynamic models indicate that further immediate transitions occur. These concepts are illustrated by analysis of phase space behavior of a hydraulic actuator.

The approach fits into our ontology for describing transition behavior in phase spaces that we have established in previous work [6]. We hope to extend this approach to systematic procedures for automated model reduction of complex nonlinear systems into simpler hybrid representations. A longer term goal of this work is to develop real time models of complex systems so that they may be employed in hybrid observers for Fault Detection and Isolation (FDI) studies of complex nonlinear systems [5].

8 Acknowledgements

Pieter J. Mosterman is supported by a grant from the DFG Schwerpunktprogramm KONDISK. Gautam Biswas is supported by grants from HP Labs, and the DARPA Software Enabled Control program.

References

1. Rajeev Alur, Costas Courcoubetis, Thomas A. Henzinger, and Pei-Hsin Ho. Hybrid automata: An algorithmic approach to the specification and verification of hybrid systems. In R.L. Grossman, A. Nerode, A.P. Ravn, and H. Rischel, editors, *Lecture Notes in Computer Science*, volume 736, pages 209–229. Springer-Verlag, 1993.

2. James Demmel and Bo Kågström. Stably computing the Kronecker structure and reducing subspaces of singular pencils $A - \lambda B$ for uncertain data. In J. Cullum and R. A. Willoughby, editors, *Large Scale Eigenvalue Problems*. Elsevier Science Publishers B.V. (North-Holland), 1986.
3. Petar V. Kokotović, Hassan K. Khalil, and John O'Reilly. *Singular Perturbation Methods in Control: Analysis and Design*. Academic Press, London, 1986. ISBN 0-12-417635-6.
4. Pieter J. Mosterman. State Space Projection onto Linear DAE Manifolds Using Conservation Principles. Technical Report #R262-98, Institute of Robotics and System Dynamics, DLR Oberpfaffenhofen, P.O. Box 1116, D-82230 Wessling, Germany, 1998.
5. Pieter J. Mosterman and Gautam Biswas. Building Hybrid Observers for Complex Dynamic Systems using Model Abstractions. In Frits W. Vaandrager and Jan H. van Schuppen, editors, *Hybrid Systems: Computation and Control*, pages 178–192, 1999. Lecture Notes in Computer Science; Vol. 1569.
6. Pieter J. Mosterman, Feng Zhao, and Gautam Biswas. An Ontology for Transitions in Physical Dynamic Systems. In *AAAI98*, July 1998.
7. A. J. van der Schaft and J. M. Schumacher. The complementary-slackness of hybrid systems. *Math. Contr. Signals Syst.*, (9):266–301, 1996.
8. Andreas Varga. On modal techniques for model reduction. Technical Report TR R136-93, Institute of Robotics and System Dynamics, DLR Oberpfaffenhofen, P.O. Box 1116, D-82230 Wessling, Germany, 1993.